EVALUATION OF THE WDD METHOD FOR THE ANALYSIS OF CORRODED PRESSURIZED PIPELINES

Paulo César Flores Cerna, flores_cerna@hotmail.com
João Elias Abdalla Filho, joao.abdalla@pucpr.br
Roberto Dalledone Machado, roberto.machado@pucpr.br
Programa de Pós-Graduação em Engenharia Mecânica, Pontifícia Universidade Católica do Paraná (PUCPR)
Rua Imaculada Conceição, 1155- Prado Velho - 80215-901, Curitiba - PR – Brasil

Abstract. *The purpose of this paper is to address the Weighted Difference Depth method (WDD) for the estimation of failure pressure of pipelines containing corrosion defects. The WDD method has been proposed several years ago. Although it is claimed to be very accurate, it lacks further validation. In this paper, the WDD method is implemented computationally in a FORTRAN code and it is applied to a set of defects in different materials used in pipeline construction. Results are compared to experimental results as well as to results provided by semi-empirical methods such as ASME B31 G, RSTRENG, DNV and PCORRC. The results presented show good accuracy and it appears that WDD is a competing method for use in practice.*

Keywords*: Pipeline, Corrosion defect assessment, WDD method, Plastic collapse*

1. INTRODUCTION

Pipelines are widely used to transport oil and gas. Thus, it is important that it operates efficiently and safely. Over time pipelines may suffer damage that can diminish its structural integrity and, consequently, cause financial losses to industries that operate them. One of the most common forms of damage present in pipelines is corrosion. The prediction of failure pressure of corroded pipes is important so that preventive actions can be taken to avoid forces that exceed their capacity and thereby enable them to remain in operation.

The first and best known research in the assessment of corrosion defects was performed by Kiefner and Vieth (1973) and resulted in what is now known as the ASME B31G criterion. The evaluation codes of corrosion defects in Canada, United States and Europe are based on this criterion. A huge improvement for B31G was introduced by Kiefner and Vieth (1989). This new iterative method was modified to evaluate the failure pressure corrosion defects using a program known as RSTRENG. New definitions for a bulging factor and material flow stress were introduced and a more detailed analysis of the shape of the corrosion was used to reduce the conservatism of the original B31G criterion.

Mok (1991) has published one of the first applications of the Finite Element Method (FEM) for analysis of corrosion defects in pipelines. This line of work was continued by Chouchaoui (1993) with experimental burst tests on pipe with isolated defects and groups of interacting defects.

Currently, both the original B31G and RSTRENG are used by pipeline operators for defect assessment. Unfortunately, the safety factor associated with these criteria is not well understood due to lack of adequate experimental data. Moreover, its application to complex defects is not well defined. The finite element method has been proposed as a less conservative approach to evaluation (Chouchaoui 1993, Fu and Kirkwood, 1995). However, it has only been validated for simple geometries of corrosion. Moreover, the cost and expertise required to perform these tests limit their use generally.

The goal of this paper is to evaluate the failure pressure of corroded pipelines with complex geometry using the Weighted Difference Depth Method (a solution procedure based on an upper and a lower limit) and compare it with currently employed evaluation methods. This procedure uses the long groove and plain pipe failure pressures as lower and upper bounds, respectively, for the defect failure pressure. The WDD Method predicts the failure pressure by interpolating between these limits based on the geometry of the corrosion. This iterative assessment technique is implemented into a FORTRAN code in the present work and it is employed in the analyses of various defect aspect ratios for different materials.

2. CODED METHODS

2.1 ASME B31G

This is a method to evaluate the residual strength of corroded pipes. It is a supplement of the ASME B31 code for pressure piping. The code was developed in the late sixties and early seventies by Battelle Memorial Institute and provides a semi-empirical procedure for the assessment of pipelines with corrosion defects. Based on an extensive series of full-scale testing of different sections, this method concluded that the toughness is not a significant factor and that failure pressure can be controlled by the size of the defect corrosion, internal pressure and the yield stress of the material.

The ASME B31G method is widely used for the assessment of corroded pipes, but has several limitations:

• Applies only to defects in the body duct which contains a uniform profile with a low stress concentration factor.

• This method does not allow assessing corrosion defects that are contained in longitudinal and circumferential welds.

• The method applies only in pipelines subjected to internal pressure, and cannot be used when presenting significant secondary loads.

The evaluation procedure considers the maximum depth and longitudinal length of the corroded surface, but does not consider the circumferential width. Input parameters include the outer pipe diameter (*D*) and wall thickness (*t*), the specified minimum yield strength (*SMYS*), the maximum allowable operating pressure (*MAOP*), the longitudinal extent of corrosion (*L*) and defect depth (*d*). The failure pressure equation for a corroded pipeline with a parabolic defect is:

Case 1: $L \leq \sqrt{20Dt}$

$$P_{ult} = \frac{2(1.1xSMYS)t}{D}\left[\frac{1-0.66\frac{d}{t}}{1-0.66\frac{d}{t}\frac{1}{M}}\right] \tag{1}$$

Case 2: $L > \sqrt{20Dt}$

$$P_{ult} = \frac{2(1.1xSMYS)\mathrm{t}}{D}\left[1-\frac{d}{t}\right] \tag{2}$$

The bulging factor is:

$$M = \sqrt{1+0.8\frac{L^2}{Dt}} \tag{3}$$

2.2 Modified ASME B31G

This includes the modified flow stress and the bulging factor. The flow stress is σ_{ult} taken as:

$$\sigma_{ult}/Mpa = 1.1\ \sigma_y + 69 \tag{4}$$

where σ_y is the yield strength. Two cases are considered for the failure pressure:

$$P_{ult} = \frac{2\sigma_{ult}}{D}\left[\frac{1-0.85\frac{d}{t}}{1-0.85\frac{d}{t}\frac{1}{M}}\right] \tag{5}$$

The bulging factor is:

Case 1: $L \leq \sqrt{50Dt}$

$$M = \sqrt{1+0.62756\frac{L^2}{Dt}-0.003375\left(\frac{L^2}{Dt}\right)^2} \tag{6}$$

Case 2: $L > \sqrt{50Dt}$

$$M = 0.032\frac{L^2}{Dt}+3.3 \tag{7}$$

The assessment procedure considers the maximum depth and longitudinal extent of the corroded area, but ignores the circumferential extent and the actual profile. If the corroded region is found to be unacceptable, B31G allows the use of a more rigorous analysis or a hydrostatic pressure test in order to determine the pipe's remaining strength. Alternatively, a lower maximum allowable operating pressure may be imposed.

2.3 DNV RP-F101

This is the first comprehensive and extensive code on pipeline corrosion defect assessment. It provides guidance on the pipeline´s internal pressure and combined loading. Furthermore, it provides a coded formulation for pressure and bending and area depth. DNV RP-F101 proposes two methods to find the failure pressure.

The first method is named as partial safety factor, and the second is classified as allowable stress design. The allowable-stress-design method which considers non-interacting defects is discussed here. To pursue the design procedure via DNV RP-F101 it is necessary to define the loading type (pressure only or combined loading), and consequently the failure pressure can be obtained as:

$$P_{ult} = \frac{2\sigma_{ult} t}{(D-t)}\left[\frac{1-\frac{d}{t}}{1-\frac{d}{t}\frac{1}{M}}\right] \tag{8}$$

$$M = \sqrt{1+0.31\left(\frac{L}{\sqrt{Dt}}\right)^2} \tag{9}$$

2.4 PCOORC

In the 1990´s, the American Gas Association (AGA) commissioned the Battelle Laboratory in order to perform a series of studies on defects in products caused by the corrosion process. On investigation, it was realized that ductile materials fail by plastic collapse; however, in the case of materials of lower hardness, failure occurs by a different mechanism and usually fail at a pressure lower than in ducts with moderate to high hardness. In addition, the study showed that the failure pressure by plastic collapse is controlled by the ultimate stress of the material instead of the flow stress. For defects that fail by plastic collapse, a finite elements based program named PCORRC was developed. The procedure furnishes corrosion defects failure analysis under the combination of internal pressure and external loading..

The finite element analysis performed by the program were compared to experimental results of BG Technology and from this an equation was obtained that defines the failure pressure in pipeline corrosion defects present in materials from high to moderate hardness. The resulting simplified criterion uses an exponential function which is given by:

$$P_{ult} = \frac{\sigma_{ult}.t}{r}\left[1-\frac{d_{max}}{t}\left(1-e^{-0.157\frac{L}{\sqrt{r(t-d)}}}\right)\right] \tag{10}$$

3. FAILURE PRESSURE IN PIPELINES

3.1. Model material

Figure 1 shows a typical engineering stress-strain curve for grade API-5L-X42. The corresponding true stress-strain curve and Ramberg-Osgood fit are also shown. It should be noted that the full stress-strain curve is not shown in Fig. 1 for clarity.

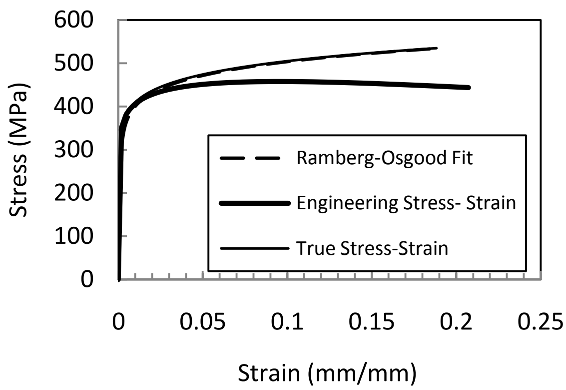

Figure 1. Engineering and true stress-strain.

The Ramberg-Osgood equation was developed to describe the nonlinear relationship between stress and strain. One of the fundamental assumptions is that accurate materials properties are available, in the form of uniaxial tensile test data. The Ramberg-Osgood material model, which relates true stress and true strain, has been found suitable to characterize pipeline steel.

$$\varepsilon = \frac{S}{E} + \alpha \frac{\sigma_{YS}}{E}\left(\frac{S}{\sigma_{YS}}\right)^{n} \tag{11}$$

Table 1 summarizes the material properties and parameters α, n that were analyzed in this study

Material Type		Ramberg-Osgood Material Parameters				Critical Stress		ε Critical
Grade	ID	σ_{YS} (MPa)	σ_{YS} (PSI)	Alpha	n	(MPa)	(PSI)	
X42	BCG	350.9	50852	3.143	8.07	506.2	73367	0.104
X46	SOL	356.7	51689	3.741	7,45	542	78557	0.15
	TCP	400.5	58050	3.007	8.34	568.2	82351	0.115
X52	NOR	389	56376	3.493	7.74	575.8	83450	0.139
	RLK	433.6	62841	1.198	10.97	603.7	87497	0.116
X55	NOV	462.7	67055	2.254	8.65	648.6	93997	0.127

3.2. Failure pressure of plain pipe

Svensson (1959) showed that homogeneous tubes made of high strength material that shows hardening behavior would amount to a geometric point of instability before reaching a level of critical stress as a result of reduced wall thickness and increased the inner radius leading to increased tension. By increasing the strain rate exceeds the rate of hardening of the material, and thus instability occurs. It is noteworthy that the strain and stress at the time of instability in the plain pipe are below critical values from a tensile test.

A solution of the instability of the plastic limit load (internal pressure) proposed by Svensson (1959) based on the theory of finite deformation plasticity and to evaluate the influence of strain hardening behavior of materials and the difference of limit loads estimated from the criterion of Tresca and Von Mises.

Svensson´s analysis was reviewed by Cronin and Pick (2002) to include the Ramberg-Osgood material model. Their result is shown in Eq. (12):

$$P_{\text{Inst}}^{n}\left[\frac{\propto}{E\sigma_{YS}^{n-1}}\left(\frac{\sqrt{3}}{2}\frac{r^2}{r_0 t_0}\right)^{n}\right] + P_{\text{Inst}}\left[\frac{\sqrt{3}}{2}\frac{r^2}{r_0 t_0 E}\right] - \frac{2}{\sqrt{3}}\ln\left(\frac{r}{r_0}\right) = 0 \tag{12}$$

Although Eq. (12) can easily be solved numerically, it does not provide a unique solution. Further, it underestimates the instability failure pressure of the plain pipe. Neglecting the elastic deformation in Eq. (12) results in a unique solution as shown in Eq. (13) to determine the pressure of instability ($P_{2\,Inst}$) as a function of the pipe material properties and geometry:

$$P_{2\,\text{Inst}} = \left(\frac{E\sigma_{YS}^{n-1}}{\sqrt{3}\propto n}\right)^{1/n}\frac{2}{\sqrt{3}}\frac{t_0}{r_0\left[\exp\left(\frac{1}{2n}\right)\right]^2} \tag{13}$$

This equation is easier to evaluate, but it underestimates the instability pressure by approximately 4% compared to the Eq. (12). In this case, $P_{Plain\ Pipe} = 0.90\text{x}P_{2Inst}$. Note that neglecting the elastic strain has a more significant effect when calculating the stress and strains in the pipe at pressures below the instability pressure.

3.3. Failure pressure of long grove corrosion defects

The simplest corrosion defect shape to considerer is a very long, longitudinally aligned groove of uniform depth. Although these defects are idealizations, they provide a lower bound for understanding the behavior of failure in pressure tubes with natural corrosion defects and the development of a new evaluation procedure. These isolated defects can be considered as simple two-dimensional defects in which the failure initiates simultaneously along the entire length of the defect. The numerical analyses made by Cronin and Pick (2002) revealed that the onset of failure can be predicted by using deformation plasticity formulation with stress-based failure criterion. The failure begins when the equivalent true stress in the defect is equal to the ultimate tensile strength of the material expressed as a true stress.

A simplified solution to determine the failure pressure in pipes with simple corrosion defects has been developed by Cronin and Pick (2002). Both equilibrium and compatibility are considered to calculate the tensile stress in the defect ligament as a function of internal pressure, initial geometry and material properties. The corresponding free-body diagram for an infinitesimal section of the groove at the ligament is shown in Fig 2. The relevant parameters of the section are the thickness (t_L), and length (w). The solid is subjected only to longitudinal (F_{Long}) and hoop (F_{Hoop}) forces.

In applying equilibrium to a structure, it is common to consider one section and replace the remainder with the appropriate boundary conditions. In the case of a simple defect, one half of the defect can be analyzed (due to symmetry) and the rest is replaced by an equivalent bending moment (M_H), forces in the circumferential direction (F_{Hoop} and F_{Plain}) and shear forces (V_H) as shown in Fig. 2. The stress in the radial direction has a maximum value at the inside surface of the pipe equal to the internal pressure which is small when compared to the hoop and longitudinal stresses and can be neglected.

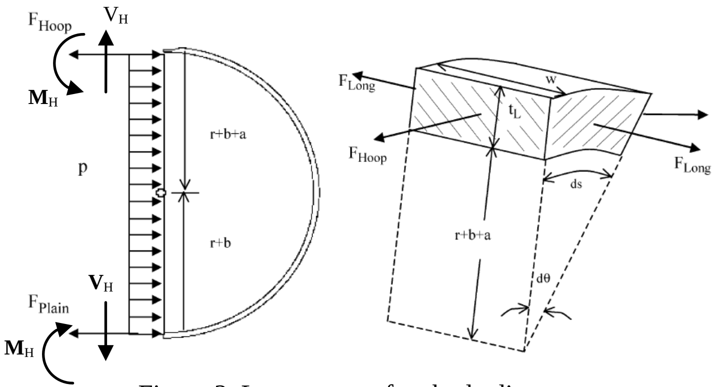

Figure 2. Long groove free body diagram

Finite element results indicate that the bending moment and shear forces tend to be very small and can be negligible (Mok, 1991). This is expected due to the high degree of plasticity. Fig. 2 shows a section of the corroded part of the plane of symmetry with a circumferential infinitesimal size (ds). In this case, the thickness is equal to the actual thickness of the ligament (t_L) in the deepest part of the defect, the section has length w, and it is subjected only to a longitudinal force (F_{Long}) and a circumferential force (F_{Hoop}).

Applying the equilibrium in the deformed geometry shown in Fig. 2, where b refers to the radial deformation of the plain pipe and a is the radial bulging of the groove,

$$F_P + F_H = pw[2(r+b)+a] \tag{14}$$

where it is assumed that:

$$F_P = pw(r+b) \quad and \quad F_H = pw(r+b+a) \tag{15}$$

Considering the moment equilibrium about the center of pressure:

$$[r+b+\frac{t}{2}]F_P = [r+b+a+\frac{t_L}{2}]F_H \tag{16}$$

Introducing Eq. (15) and neglecting second order terms, Eq. (16) simplifies to:

$$a = a_{max} = \frac{(t-t_L)}{4} \tag{17}$$

The assumption of incompressibility during plastic flow, and plane strain condition requires that:

$$\sigma_{\mathrm{Long}} = \frac{1}{2}\sigma_{\mathrm{Hoop}} \tag{18}$$

Assuming that the longitudinal stress is due to the internal pressure. Then the equivalent Von Mises stress in the ligament can be expressed in terms of the ligament hoop forces as:

$$\sigma_{\mathrm{Mises}} = \sqrt{\frac{3}{2}(s_1^2+s_3^2)} = \sqrt{\frac{3}{2}\left[\left(\frac{1}{2}\frac{\mathrm{F_{Hoop}}}{\mathrm{wt_L}}\right)^2 + \left(-\frac{1}{2}\frac{\mathrm{F_{Hoop}}}{\mathrm{wt_L}}\right)^2\right]} = \sqrt{\frac{3}{4}}\frac{\mathrm{F_{Hoop}}}{wt_{\mathrm{L}}} \quad \text{or} \quad \mathrm{F_{Hoop}} = \frac{\sigma_{\mathrm{UTS}}}{\sqrt{\frac{3}{4}}}wt_{\mathrm{L}} \tag{19}$$

Where S_1 and S_3 are the components of deviatoric stresses and S_2 =0.

At failure, the average ligament strain is equal to the equivalent true strain corresponding to the ultimate tensile strength of the material. Due to the large degree of plasticity, it is assumed that the material is incompressible:

$\varepsilon_{Thick} + \varepsilon_{Hoop} + \varepsilon_{Long} = 0$, so $-\varepsilon_{Thick} = \varepsilon_{Hoop}$, and from the equations the Von Mises effective strain is:

$$\bar{\varepsilon} = \sqrt{\frac{4}{3}}\varepsilon_{\mathrm{Hoop}} = -\sqrt{\frac{4}{3}}\varepsilon_{\mathrm{Thick}} = -\sqrt{\frac{4}{3}}\ln\left(\frac{t_L}{t_0}\right) \tag{20}$$

Note that the negative sign in Eq. (19) is necessary to produce a positive equivalent strain since the thickness strain is negative. At failure, the stress and strain state corresponds to that of the ultimate tensile strength, and strain and stress are expressed as true quantities, so:

$$\varepsilon_{\mathrm{UTS}} = -\sqrt{\frac{4}{3}}\ln\left(\frac{t_L}{t_0}\right) \qquad \text{or} \qquad t_L = t_0 \exp\left(-\sqrt{\frac{3}{4}}\varepsilon_{\mathrm{UTS}}\right) \tag{21}$$

where t_L is the ligament thickness at failure. From the Eq. (15) and (21) we can express the failure pressure of a long groove as:

$$p_{Long\ Groove}\left[r + b + \frac{(t - t_L)}{4}\right] - \frac{\sigma_{\mathrm{UTS}}}{\sqrt{\frac{3}{4}}} t_{L0} \exp\left(-\sqrt{\frac{4}{3}}\varepsilon_{\mathrm{UTS}}\right) = 0 \tag{22}$$

Here *b* and *t* are found from the plain pipe solution for the given pressure. Eq. (12) and (22) must be solved together in an iterative manner. However, assuming that the plain pipe deformation (b) and defect bulging (a) are insignificant compared with the tube radius, Eq. (22) can be expressed as:

$$p_{Long\ Groove} = \frac{\sigma_{\mathrm{UTS}}}{r\left(\sqrt{\frac{3}{4}}\right)} t_{L0} \exp\left(-\sqrt{\frac{4}{3}}\varepsilon_{\mathrm{UTS}}\right) = 0, \quad \frac{t_{L0}}{t_0} \geq 0.2 \tag{23}$$

4. WEIGHTED DIFFERENCE DEPTH METHOD

The failure pressure of a pipe with corrosion defects can be bounded by the failure pressure of a plain pipe ($P_{\mathrm{Plain\ Pipe}}$- upper limit) and the failure pressure of a pipe with corrosion defects longitudinally oriented ($P_{\mathrm{Long\ Groove}}$ - lower limit). The Weighted Difference Depth (WDD) method estimates the failure pressure by interpolating between these limits along the corrosion geometry. Based on these limits, the failure pressure (P_{Failure}) of a corrosion defect can be expressed as shown:

$$P_{\mathrm{Failure}} = P_{\mathrm{Long\ Groove}} + \left(P_{\mathrm{Plain\ Pipe}} - P_{\mathrm{Long\ Groove}}\right) \mathrm{x}\ \mathrm{g} \tag{24}$$

The parameter g varies from 0.0 to 1.0, and it is a function of corrosion and pipe geometry. Observations and analyses of real corrosion defects (Cronin and Pick, 2002) suggest that the function g should incorporate some specific characteristics:

• The failure of a corrosion defect initiates at some point that is not necessarily the point with maximum depth of the defect. The WDD method considers each point of the defect to determine the location of failure.

• The effect of adjacent corrosion on the evaluation point decreases with increasing longitudinal separation. Once the pipe is a continuous body, it should be expected that the effect of adjacent wall loss be weighted according to the longitudinal distance between the points of evaluation.

• The corrosion defect can be considered as metal loss projected onto the longitudinal axis of the pipe. This is known as the projection method. Once the defect is projected onto a plane, all calculations will be depending on the corresponding area.

It is necessary to consider the geometry of the corrosion defect. In RSTRENG B31G, the geometric effect of corrosion appears as the ratio of the ligament area to the original area. This relationship is recognized as an appropriate way to quantify the reduction in strength due to the presence of corrosion and it is expressed in Eq. (25) where *dz* is an infinitesimal length in the longitudinal direction as shown in Fig. 3

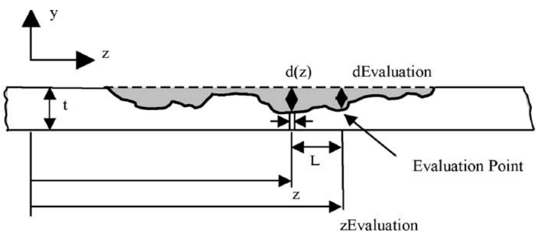

Figure 3(a). Corrosion evaluation parameter.

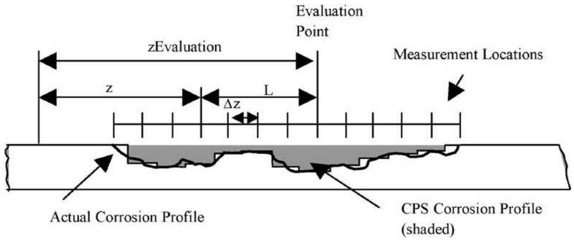

Figure 3(b). Actual corrosion profile.

$$\frac{\text{ligament Area}}{\text{Original Area}} = \frac{(t_0 - d)dz}{t_0 dz} = 1 - \frac{d}{t_0} \tag{25}$$

At an evaluation point in Fig. 3(b), the failure pressure is influenced by adjacent corrosion, weighted by the distance from the evaluation point. WDD uses the hyperbolic secant as function to weight the effects of corrosion to a normalized longitudinal distance Q from the point of evaluation. This function is appropriate since it has an exponential decay about the evaluation point. Thus, increasing the distance from the evaluation point results in a decreased weighting for adjacent areas of corrosion.

$$\text{Sech}\,(Q) = \frac{2}{e^{Q} + e^{-Q}}, \qquad \textit{where} \qquad Q = \frac{L}{\text{Normalizaton factor}} = \frac{Z_{\text{evaluation}} - Z}{\text{Normalizaton factor}} \tag{26}$$

Batte (1997) suggested that the length can be normalized by the factor of $\sqrt{Dt}$

Stephens and Leis (2000) used a normalization factor $\sqrt{r(t - d_{max})}$ based on the defect depth, but the FEM analysis results demonstrate to be more appropriate to consider the diameter. Hence,

$$\text{Sech}\,(Q) = \text{Sech}\left[\frac{Z_{\text{evaluation}} - Z}{\sqrt{D(t - d_{max})}}\right] \tag{27}$$

The effect of adjacent corrosion on the evaluation can be described in terms of the difference in the remaining ligament ratio as shown in Eq. (28):

$$\text{Depth Difference} = \left[1 - \frac{d}{t_0}\right] - \left[1 - \frac{d_{\text{evaluation}}}{t_0}\right] \tag{28}$$

The effect of corrosion at a distance L from the point of evaluation can be described as:

$$\text{WDD} = \text{Sech}\left[\frac{Z_{\text{evaluation}} - Z}{\sqrt{D(t - d_{max})}}\right]\left[\left(1 - \frac{d}{t_0}\right) - \left(1 - \frac{d_{\text{evaluation}}}{t_0}\right)\right] \tag{29}$$

Where Z is the current position and $Z_{evaluation}$ is the location of the evaluation point from the arbitrary origin *Z*.

The defect is characterized by a number of depth measurements taken at uniform interval (*ΔZ*) along the length of the defect. For a set of *n* measurements, the corrosion defect can be evaluated by the approximation of the integral as a summation as shown in Eq. (31):

$$\text{Sum WDD} = \sum_{i=1}^{i=n} \text{WDD} = \sum_{i=1}^{i=n}\left\{\text{Sech}\left[\frac{Z_{\text{evaluation}} - Z}{\sqrt{D(t - d_{max})}}\right]\left[\left(1 - \frac{d}{t_0}\right) - \left(1 - \frac{d_{\text{evaluation}}}{t_0}\right)\right]\Delta Z\right\} \tag{30}$$

For defects with a uniform depth, Eq. (30) is equal to zero. Similarly, for defects with no depth (plain pipe), Sum WDD is zero. For real corrosion defects, Eq. (30) can take on values between 0.0 and a maximum (Max WDD) which corresponds to the weighted difference of the plain pipe with respect to the current evaluation depth. The maximum weighted difference is calculated from Eq. (31) where the depth is set to 0.0 corresponding to plain pipe at all locations except at the evaluation point:

$$\mathrm{Max.WDD} = \sum_{i=1}^{i=n} \mathrm{WDD} = \sum_{i=1}^{i=n} \left\{ \mathrm{Sech}\left[\frac{Z_{\mathrm{evaluation}} - Z}{\sqrt{D(t - d_{\max})}}\right]\left[\left(1 - \frac{0.0}{t_0}\right) - \left(1 - \frac{d_{\mathrm{evaluation}}}{t_0}\right)\right] \Delta Z \right\} \tag{31}$$

If function g is defined as the ratio of the *Sum WDD* to *Max WDD*, it can theoretically vary between 0.0 and 1.0:

$$g = \frac{\mathrm{Sum.WDD}}{\mathrm{Max.WDD}} \tag{32}$$

A value of 1.0 for g is a theoretical limit, which is not achieved for real defects. As the defect depth decreases and the wall thickness approaches that of a plain pipe, the long groove solution converges to the plain pipe solution. Substituting Eq. (32) into Eq. (24), the failure pressure of a corrosion defect, evaluated at a specific point, is:

$$P_{\mathrm{Failure}} = P_{\mathrm{Long\ Groove}} + \left(P_{\mathrm{Plain\ Pipe}} - P_{\mathrm{Long\ Groove}}\right) \mathrm{x}\ \frac{\mathrm{Sum.WDD}}{\mathrm{Max.WDD}} \tag{33}$$

Eq. (33) must be evaluated at each point of the defect to determine the location with minimum failure pressure. For the case of a single pit, this will always occur in the deepest cavity. However, this may not be the case for natural corrosion defects where failure can initiate at locations other than the deepest point in the defect depending on the geometry of the surrounding corrosion.

.

5. RESULTS

The results provided by the WDD method show acceptable degrees of accuracy with a minimum percent error of 0.372% (X46 material) and a maximum one of 20.15% (X42 material).

Figure 4, 5 and 6 shows the failure pressure predictions for physically tested pipe specimens (X42, X46, X52 and X55 materials) obtained using WDD method and semi-empirical evaluation techniques, namely; ASME B31G, 0.85dL, PCOORC and DNV-RP-F101. These results clearly reveal that the ASME B31G and 0.85 dL methods are more conservative.

In all cases analyzed, results show that WDD method has improved accuracy with increasing defect depth which is consistent with DNV and PCOORC solutions.

According to the plots in the aforementioned figures, WDD results approach the experimental ones as lower bounds. As opposed to semi-empirical techniques, failure pressures provided by the WDD method do not overestimate experimental failure pressures. Figure 4(a) and figure 4(b) show that the DNV method overestimates the failure pressure for a given range of d/t values in approximately 13,0 % while the PCOORC method overestimates it in approximately 8,5 %. The WDD curves in the figures show that the WDD method underestimates failure pressures in an average percent error which ranges from 13,0 % to 20,0 %.

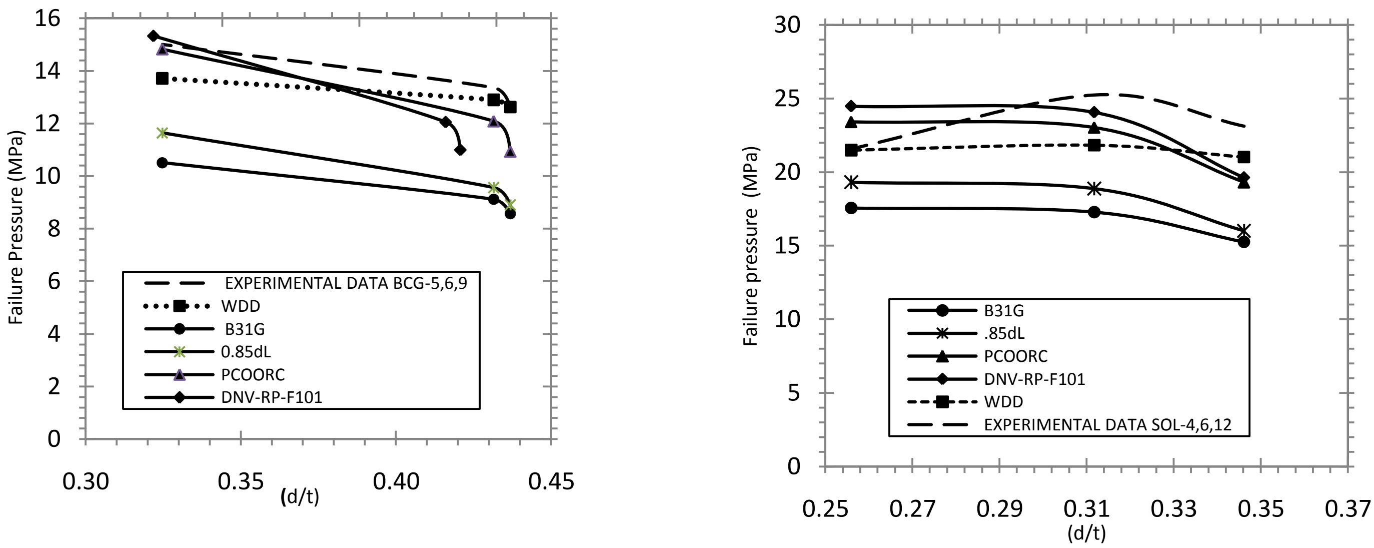

(a) (b)

Figure 4 Comparison of failure pressure prediction between WDD and DNV, PCOORC, 0.85dL, B32G: (a) X42 pipe specimens; (b) X46 pipe specimens.

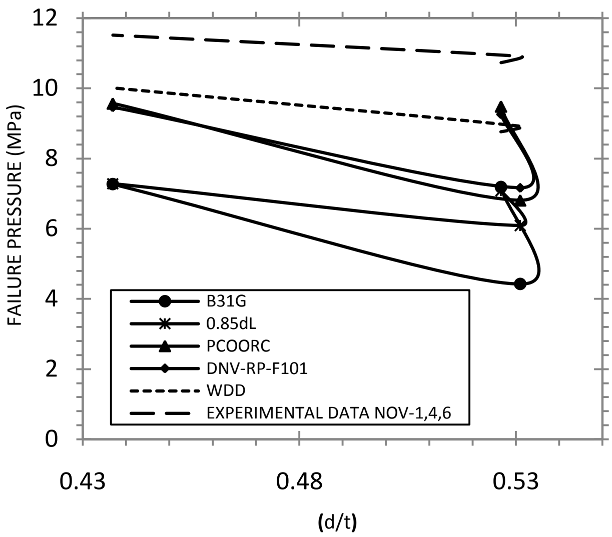

(a)

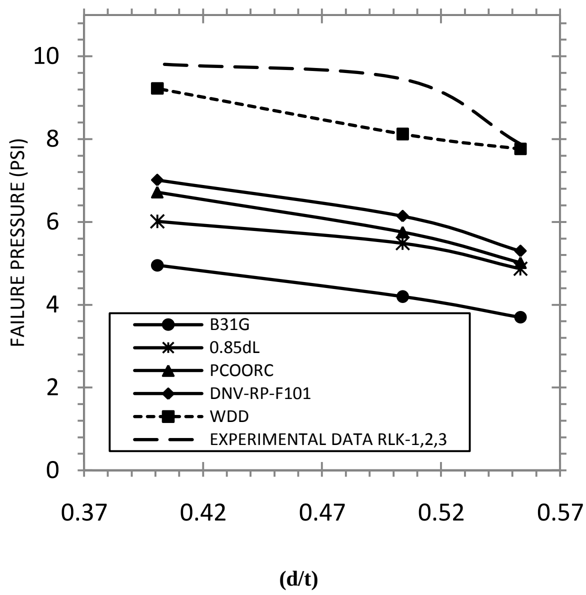

(b)

Figure 5 Comparison of failure pressure prediction between WDD and DNV, PCOORC, 0.85dL, B32G: (a) X5 pipe specimens; (b) X55 pipe specimens.

Further, Figure 6 shows the failure pressure prediction for plain pipes. In this case, the parameter *g* is zero and WDD method calculates the failure pressure of plain pipe. The method overestimates the experimental failure pressure by approximately 4,3 %, which is lower than results provided by DNV and PCOORC which overestimates the experimental data by 8,9 % and 5,9 %, respectively. Figure 6 also shows that the ASME B31G and Modified B31G (or 0.85 dL) underestimated the failure pressure by an average of 24,0 % and 13,0 %, respectively.

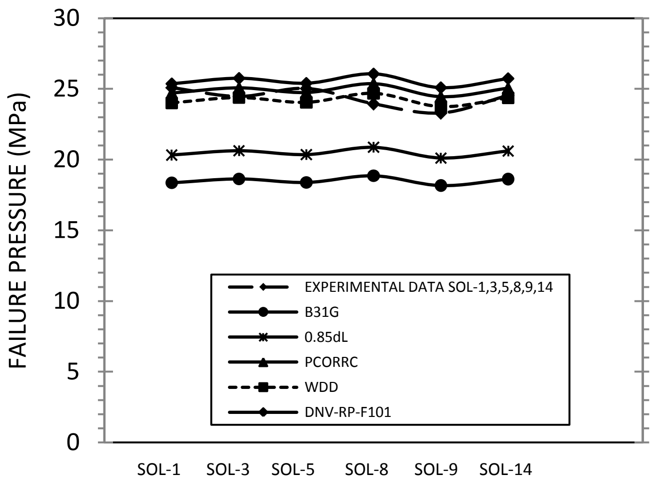

Figure 6. Failure pressure of plain pipe for 6 burst tests.

6. CONCLUSIONS

The Weighted Depth Difference Method proposed by Cronin and Pick (2002) for predicting the failure pressure of pipelines containing complex corrosion defects has been reviewed in order to demonstrate whether the method is accurate when compared to other techniques. This method employs an iterative procedure that accounts for the depth variability of the corrosion defect profile and it is applicable to any corrosion defect shape and material type as long as the failure is ductile in nature. The long groove and plain pipe solutions are used as lower and upper bounds, respectively, for the defect failure pressure.

Analyses have been performed for various API materials and corrosion defects. Results were compared to experimental results provided by Cronin and Pick (2002) and to analytical results provided by semi-empirical methods. The Weighted Depth Difference method has been shown to be sufficiently accurate as its results approach reasonably well the experimental ones. Actually, the WDD method performance has been comparable, and in some instances superior, to those of the semi-empirical techniques. The advantage of WDD over the other techniques is its capability of modeling the irregularities of the corrosion profile.

The WDD method has been validated here only against the experimental data obtained at the University of Waterloo by Cronin and Pick (2002). This is why API-X55 is the highest strength material employed. Additional experimental database on other materials would be desirable to extend the validation of this assessment procedure.

7. ACKNOWLEDGEMENTS

The authors would like to acknowledge the scholarship provided by CAPES (Brazilian agency) to the second author during his master´s degree studies, allowing this research work to be conducted.

8. REFERENCES

API, 2000. "Specification for Line Pipe – Specification 5L", 42th edition, American Petroleum Institute, Washington.

ASME, 1991. "Manual for Determining the Remaining Strength of Corroded Pipelines – A Supplement to ASME B31 Code for Pressure Piping", The American Society of Mechanical Engineers, New York.

Batte, A. D., Fu, B., Kirkwood, M. G., Vu, D., 1997. "New methods for determining the remaining strength of corroded pipeline", OMAE, V: 221-8

Benjamin, A. C. and Andrade, E. Q., 2004. "Structural Evaluation of Corrosion Defects in Pipelines: Comparison of FE Analyses and Assessment Methods", Proc. 14th International Offshore and Polar Engineering Conference, ISBN 1 880653-62-1, ISSN 1098-6189, Toulon.

Choi, J. B., Goo, B. K.; Kim, J.C., et al., 2003. "Development of Limit Load Solutions for Corroded Gas Pipelines", International Journal of Pressure Vessels and Piping 80, pp 121–128

Chouchaoui, B. A. and Pick, R. J., 1994. "A Three Level Assessment of Residual Strength of Corroded Line Pipe", Proc. OMAE 94, 13th International Conference on Offshore Mechanics and Arctic Engineering, v.5, Pipeline Technology, pp.9-18.

Cronin, D. S. and Pick, R. J, 2002. " Prediction of the Failure Pressure for Complex Corrosion Defects", International Journal of Pressure Vessels and Piping 79, pp. 279–287.

DNV, 2004. "DNV Recommended Practice – DNV–RP–F101 - Corroded Pipelines", Det Norske Veritas, Norway.

Grigory, S. C; Smith, M. Q, 1996. " Residual Strength of 48-Inch Diameter Corroded Pipe Determined by Full Scale Combined Loading Experiments", Proc. International Pipeline Conference, ASME, Vol.1, pp. 377-386.

Grigory, S. C., Smith, M. Q.; et al., 1996. "The Development of Methodologies for Evaluating the Integrity of Corroded Pipelines Under Combined Loading – Part 1: Experimental Testing and Numerical Simulations", Proc. Energy Week' 96, Book 2, Terminals and Storage, pp.58-66.

Grigory, S. C; Smith, M. Q.; et al., 1996. "The Development of Methodologies for Evaluating the Integrity of Corroded Pipelines under Combined Loading – Part 2: Engineering Model and PC Program Development", Proc. Energy Week' 96, Book 2, Terminals and Storage, pp.67-76.

Kiefner, J.F.; Vieth, P.H.; Roytman I., 1996. "Continued Validation of RSTRENG", Contract PR218-9304, Pipeline Research Committee, American Gas Association.

Kiefner, J. F.; Vieth, P. H., 1989. " A Modified Criterion for Evaluating the Remaining Strength of Corroded Pipe", Final Report on Project PR3-805, Pipeline Research Committee, American Gas Association.

Mok, D. H. B., Pick, R. J., Glover, A. J., Hoff, R., 1991. "Bursting of line pipe with long external corrosion", International Journal of Pressure Vessels and Piping 46, pp. 195-215.

Roy, S. et al., 1997. "Numerical Simulations of Full-Scale Corroded Pipe Tests with Combined Loading", Journal of Pressure Vessel Technology, v.119, pp. 457-466.

Stephens, D. R. and Leis, B. N, 2000. "Development of an Alternative Criterion for Residual Strength of Corrosion Defects in Moderate-to High-Toughness Pipe", Proc. Int. Pipeline Conference, ASME, Vol. 2, pp. 781-792.

Svensson, N.L., 1959. "The bursting pressure on cylindrical and spherical vessels", ASME, Pres. Ves. Piping Des.